Author Manuscript

Author Manuscript

Author Manuscript

Author Manuscript

HHS Public Access

Author manuscript

J Comp Neurol. Author manuscript; available in PMC 2015 September 28.

Published in final edited form as:

J Comp Neurol. 2011 March 1; 519(4): 790–805. doi:10.1002/cne.22550.

Cholinergic Innervation of Pyramidal Cells and Parvalbumin-Immunoreactive Interneurons in the Rat Basolateral Amygdala

Jay F. Muller, **Franco Mascagni**, and **Alexander J. McDonald***

Department of Pharmacology, Physiology and Neuroscience, University of South Carolina School of Medicine, Columbia, South Carolina 29208

Abstract

The basolateral nucleus of the amygdala receives an extremely dense cholinergic innervation from the basal forebrain that is critical for memory consolidation. Although previous electron microscopic studies determined some of the postsynaptic targets of cholinergic afferents, the majority of postsynaptic structures were dendritic shafts whose neurons of origin were not identified. To make this determination, the present study analyzed the cholinergic innervation of the anterior subdivision of the basolateral amygdalar nucleus (BLa) of the rat using electron microscopic dual-labeling immunocytochemistry. The vesicular acetylcholine transporter (VAChT) was used as a marker for cholinergic terminals; calcium/calmodulin-dependent protein kinase II (CaMK) was used as a marker for pyramidal cells, the principal neurons of the BLa; and parvalbumin (PV) was used as a marker for the predominant interneuronal subpopulation in this nucleus. $VAChT^+$ terminals were visualized by using diaminobenzidine as a chromogen, whereas $CAMK^+$ or PV^+ neurons were visualized with Vector very intense purple (VIP) as a chromogen. Quantitative analyses revealed that the great majority of dendritic shafts receiving cholinergic inputs were $CAMK^+$, indicating that they were of pyramidal cell origin. In fact, 89% of the postsynaptic targets of cholinergic terminals in the BLa were pyramidal cells, including perikarya (3%), dendritic shafts (47%), and dendritic spines (39%). PV^+ structures, including perikarya and dendrites, constituted 7% of the postsynaptic targets of cholinergic axon terminals. The cholinergic innervation of both pyramidal cells and PV^+ interneurons may constitute an anatomical substrate for the generation of oscillatory activity involved in memory consolidation by the BLa.

INDEXING TERMS

vesicular acetylcholine transporter; calcium/calmodulin-dependent protein kinase II; immunocytochemistry; electron microscopy; acetylcholine

The basal forebrain contains an array of cholinergic neurons that extends through a continuous region that includes the medial septal area, diagonal band, ventral pallidum, and substantia innominata. Different portions of this complex have connections with different forebrain regions, including the hippocampus, neocortex, and basolateral nuclear complex of

*CORRESPONDENCE TO: Alexander J. McDonald, PhD, Department of Pharmacology, Physiology and Neuroscience, University of South Carolina School of Medicine, Columbia, SC 29208. alexander.mcdonald@uscmed.sc.edu.

Author Manuscript Author Manuscript Author Manuscript Author Manuscript

the amygdala (BLC; Mesulam et al., 1983a,b; Zaborszky et al., 1999). The BLC in the rat, monkey, and human receives an especially dense cholinergic innervation from the ventral pallidum and substantia innominata, which is significantly reduced in Alzheimer's disease (Mesulam et al., 1983a,b; Carlsen et al., 1985; Carlsen and Heimer 1986; Amaral and Bassett, 1989; Kordower et al., 1989; Emre et al., 1993). In fact, it has been suggested that the degeneration of the cholinergic projections to the amygdala in Alzheimer's disease may be more important for the memory disturbances seen in this disorder than the cholinergic projections to the cortex (Power et al., 2003). Experiments in rats have demonstrated that cholinergic afferents to one specific BLC nucleus, the anterior subdivision of the basolateral nucleus (BLa), are primary mediators of the neuromodulation involved in memory consolidation of emotionally arousing experiences by the amygdala (McGaugh, 2004). Cholinergic projections to the BLC have also been implicated in fear conditioning (Vazdarjanova and McGaugh, 1999), reward devaluation learning (Salinas et al., 1997), conditioned place preference (McIntyre et al., 2002), and conditioned cue reinstatement of drug seeking (See, 2005).

Knowledge of the cholinergic innervation of specific cell types in the BLC is critical for understanding the physiology and pathophysiology of these important inputs. Previous studies have shown that there are two major cell classes in the BLC, pyramidal neurons and non-pyramidal neurons. Although these cells do not exhibit a laminar or columnar organization, their morphology, synaptology, electrophysiology, and pharmacology are remarkably similar to those of their counterparts in the cerebral cortex (McDonald, 1982, 1984, 1992a,b; Carlsen and Heimer, 1988; Washburn and Moises, 1992; Rainnie et al., 1993; Paré, 2003; Sah et al., 2003; Muller et al., 2005, 2006, 2007). Thus, pyramidal neurons in the BLC are projection neurons with spiny dendrites that utilize glutamate as an excitatory neurotransmitter, whereas most nonpyramidal neurons are spine-sparse interneurons that utilize GABA as an inhibitory neurotransmitter. Recent dual-labeling immunohistochemical studies suggest that the BLC contains at least four distinct subpopulations of GABAergic interneurons that can be distinguished on the basis of their content of calcium-binding proteins and peptides. These subpopulations are: 1) parvalbumin$^+$/calbindin$^+$ neurons; 2) somatostatin$^+$/calbindin$^+$ neurons; 3) small bipolar and bitufted inter-neurons that exhibit extensive colocalization of vasoactive intestinal peptide, calretinin, and cholecystokinin; and 4) large multipolar cholecystokinin$^+$ neurons that are often calbindin$^+$ (Kemppainen and Pitkänen, 2000; McDonald and Betette, 2001; McDonald and Mascagni, 2001, 2002, Mascagni and McDonald, 2003).

There is evidence from electrophysiological studies that basal forebrain cholinergic inputs activate both pyramidal projection neurons and GABAergic interneurons in the BLa by both muscarinic (Washburn and Moises, 1992; Yajeya et al., 1997; Pape et al., 2005; Power and Sah, 2008) and nicotinic (Zhu et al., 2005; Klein and Yakel, 2006) receptor-mediated mechanisms. Consistent with these findings, ultrastructural analyses of the BLa revealed synaptic contacts of cholinergic (i.e., choline acetyltransferase-positive) axons with both major neuronal classes (Carlsen and Heimer, 1986; Nitecka and Frotscher, 1989). Carlsen and Heimer (1986) found that some cholinergic axons formed synapses with cell bodies of BLa pyramidal neurons that were identified either morphologically or by virtue of their labeling by injections of retrograde tracers into the ventral striatum. However, most synaptic

Author Manuscript Author Manuscript Author Manuscript Author Manuscript

contacts were seen with unlabeled dendritic shafts and to a lesser extent with dendritic spines (Carlsen and Heimer, 1986). Cholinergic synaptic inputs were also seen targeting BLa interneurons that were identified either morphologically (Carlsen and Heimer, 1986) or by virtue of their immunohistochemical labeling for GAD (Nitecka and Frotscher, 1989) or choline acetyltransferase (Carlsen and Heimer, 1986). Because neither of these two ultrastructural analyses used quantitative methods, and because neither labeled the great majority of dendritic shafts, the major targets of cholinergic synaptic inputs to the BLa, there is currently no information regarding the postsynaptic targets of the majority of cholinergic inputs to this brain region.

The present dual-labeling EM study addressed this issue by using antibodies to the vesicular acetylcholine transporter (VAChT) to label cholinergic axons (Weihe et al., 1996; Gilmor et al., 1996) and antibodies to cell-specific markers to identify different neuronal subpopulations in the BLa. An antibody to the alpha subunit of calcium/calmodulin kinase II (CaMK) was used to label pyramidal cell perikarya and dendrites (McDonald et al., 2002), and an antibody to parvalbumin (PV) was used to label this important subpopulation of interneurons. PV^+ interneurons are the predominant subpopulation in the BLa, making up approximately 40% of all interneurons (McDonald and Mascagni, 2001; Mascagni and McDonald, 2003). In addition, the nonaccommodating, rapid firing pattern of many PV^+ neurons (Rainnie et al., 2006; Woodruff and Sah, 2007a) indicates that they correspond to many of the interneurons identified in previous electrophysiological studies of cholinergic activation of the BLa (Washburn and Moises, 1992; Zhu et al., 2005).

MATERIALS AND METHODS

Tissue preparation

All experiments were performed in male Sprague-Dawley rats (250–350 g; Harlan) and were carried out in accordance with the NIH principles of laboratory animal care (NIH publication no. 86-23, revised 1985). All procedures were approved by the University of South Carolina Institutional Animal Care and Use Committee. For light microscopy, rats (n = 5) were anesthetized with chloral hydrate (350 mg/kg) and perfused intracardially with phosphate-buffered saline (PBS; pH 7.4) containing 0.5% sodium nitrite (50 ml), followed by 4% paraformaldehyde in phosphate buffer (PB; pH 7.4; 500 ml). Brains were removed and postfixed in the perfusate for 3 hours. For electron microscopy, rats (n = 8) were anesthetized and perfused intracardially with PBS containing 0.5% sodium nitrite (50 ml), followed by an acrolein/paraformaldehyde mixture (2.0% paraformaldehyde-3.75% acrolein in PB for 1 minute, followed by 2.0% paraformaldehyde in PB for 30 minutes). After removal, acrolein-fixed brains were postfixed in 2.0% paraformaldehyde for 1 hour. Two additional rats received bilateral injections of colchicine (100 μg total; Sigma, St. Louis, MO) into the lateral cerebral ventricles 1 day before acrolein/paraformaldehyde perfusion to determine whether blockade of axonal transport might produce VAChT immunoreactivity in BLC interneurons. These brains were processed for light microscopy only.

Brains were sectioned on a vibratome in the coronal plane at either 50 μm (for light microscopy) or 60 μm (for electron microscopy). Sections from acrolein-fixed brains were rinsed in 1.0% borohydride in PB for 30 minutes and then rinsed thoroughly in several

Author Manuscript Author Manuscript Author Manuscript Author Manuscript

changes of PB for 1 hour. Sections were processed for immunocytochemistry in the wells of tissue culture plates.

Light microscopic immunocytochemistry

Antibodies are listed in Table 1. Single-label localization of vesicular acetylcholine transporter (VAChT) was performed in seven rats (five perfused with 4% paraformaldehyde and two perfused with the acrolein/paraformaldehyde mixture after colchicine injection; see above) using a goat polyclonal antibody to VAChT (1:10,000; catalog No. 24286; Immunostar, Hudson, WI). All antibodies were diluted in PBS containing 0.3% Triton X-100 and 1% normal donkey serum (NDS). Sections were incubated in primary antibody overnight at 4°C and then processed for the avidin-biotin immunoperoxidase technique using a biotinylated donkey anti-goat secondary antibody (1:400; Jackson Immunoresearch Laboratories, West Grove, PA) and a Vectastain standard ABC kit (Vector Laboratories, Burlingame, CA). Nickel-enhanced DAB (3,3′-diaminobenzidine-4HCl; Sigma) was used as a chromogen to generate a black reaction product (Hancock, 1986). After the immunohistochemical procedures, sections were mounted on gelatinized slides, dried overnight, dehydrated in ethanol, cleared in xylene, and coverslipped in Permount (Fisher Scientific, Pittsburgh, PA). In one of the five noncolchicine-injected rats, sections were Nissl counterstained with 1% pyronin Y to label neuronal somata in the amygdala. Sections were analyzed with an Olympus BX51 microscope, and digital light micrographs were taken with an Olympus DP2-BSW camera system. Brightness and contrast were adjusted in Photoshop 6.0 software.

Electron microscopic double-label immunocytochemistry

Electron microscopic immunocytochemistry using a sequential dual-labeling immunoperoxidase method (Muller et al., 2006) was utilized in eight rats to survey the cholinergic innervation of neurons in the anterior subdivision of the basolateral nucleus (BLa; bregma levels –2.1 through –2.6; Paxinos and Watson, 1997). The BLa was chosen for study because it receives the densest cholinergic innervation in the amygdala and because cholinergic inputs from the basal forebrain to the BLa are critical for memory consolidation of emotionally arousing experiences (McGaugh, 2004).

Sections were cryoprotected in 30% sucrose in PB for 3 hours, followed by three cycles of freezing-thawing over liquid nitrogen in order to increase antibody penetration. Sections were then rinsed well in PB and incubated for 36 hours at 4°C in the goat VAChT antibody (1:6,000) in PBS containing 1% NDS and processed using a biotinylated donkey anti-goat secondary antibody (1:400; Jackson Immunoresearch Laboratories) and a Vectastain standard ABC kit (Vector Laboratories) with nonintensified DAB as the chromogen. After rinsing, sections were incubated in a avidin/biotin blocking solution (avidin/biotin blocking kit; Vector Laboratories). Sections were then incubated overnight at 4°C in either mouse anti-CaMK (1:500; Sigma) to label pyramidal cells (McDonald et al., 2002; Muller et al., 2006, 2007) or in rabbit anti-PV (1:6,000; donated by Dr. Kenneth Baimbridge, University of British Columbia) to label the PV^+ interneuronal subpopulation (McDonald and Mascagni, 2001). PV^+ interneurons were chosen for analysis because 1) they represent the predominant interneuronal subpopulation in the BLa (Mascagni and McDonald, 2003); 2)

Author Manuscript Author Manuscript Author Manuscript Author Manuscript

both somata and dendrites, including distal dendrites, are intensely stained; and 3) the nonaccommodating, rapid firing pattern of many PV^+ neurons (Rainnie et al., 2006; Woodruff and Sah, 2007a) indicates that they correspond to many of the interneurons identified in previous electrophysiological studies of cholinergic activation of the BLa (Washburn and Moises, 1992; Zhu et al., 2005). For CaMK immunoreactivity, sections were processed using a biotinylated donkey anti-mouse secondary antibody (1:200; Jackson Immunoresearch Laboratories) and an Elite ABC kit (Vector Laboratories). For PV immunoreactivity, sections were then processed using a biotinylated donkey anti-rabbit secondary antibody (1:400; Jackson Immunoresearch Laboratories) and a Vectastain standard ABC kit (Vector Laboratories). PV and CaMK immunoreactivity was then visualized by using a Vector-VIP (very intense purple) peroxidase substrate kit (V-VIP; Vector Laboratories). This procedure yields a reaction product that appears purple in the light microscope and granular or particulate in the electron microscope (Smiley et al., 1997; Van Haeften and Wouterlood, 2000; Muller et al., 2005). For electron microscopy, the penetration of the V-VIP reaction was similar to that of DAB immunoperoxidase, and the particulate reaction product was easily distinguishable from the dense, diffuse DAB immunoperoxidase reaction product.

Sections processed for electron microscopy were postfixed in 2% osmium tetroxide in 0.16 M sodium cacodylate buffer (pH 7.4) for 1 hour, dehydrated in graded ethanols and acetone, and flat embedded in Polybed 812 (Polysciences, Warrington, PA) in slide molds between sheets of Aclar (Ted Pella, Redding, CA). Steps in the dehydration series were shortened by 25–30% to minimize extraction of the purple reaction product (Lanciego et al., 1997). Selected areas of the BLa were remounted onto resin blanks. Silver thin sections were collected on formvar-coated slot grids, stained with uranyl acetate and lead citrate, and examined with a JEOL-200CX electron microscope. Micrographs were taken with an AMT XR40 digital camera system (Advanced Microscopy Techniques, Danvers, MA). For publication, figures were then assembled and labeled and their components' tonal ranges adjusted and matched in Adobe Photoshop 6.0.

Analysis

Data analysis focused on the synaptic contacts formed by $VAChT^+$ axon terminals with PV^+ and $CaMK^+$ structures (one or two vibratome sections per animal in four animals were analyzed for each pair of neuronal markers). Serial sections were analyzed and often followed on consecutive grids. Serial sections were helpful for verifying label in small and lightly immunoreactive structures, determining the synaptic nature of contacts, and identifying multiple targets of individual $VAChT^+$ terminals. Synapses were identified by standard criteria: 1) parallel pre-synaptic and postsynaptic membranes exhibiting membrane thickenings, 2) a synaptic cleft containing dense material, and 3) clustered synaptic vesicles associated with the presynaptic membrane (Peters et al., 1991). Asymmetrical and symmetrical synapses were identified based on the presence or absence, respectively, of a prominent postsynaptic density and on the relative widths of their synaptic clefts. Whereas synaptic clefts of asymmetrical synapses are typically 20 nm wide, symmetrical synapses have a much narrower synaptic cleft that is only about 12 nm wide (Peters et al., 1991). Similar to many GABAergic symmetrical synapses in the cerebral cortex (see, e.g., Fig.

Author Manuscript Author Manuscript Author Manuscript Author Manuscript

11-9 of Peters et al., 1991), the postsynaptic densities of many symmetrical synapses formed by VAChT$^+$ terminals in the BLa were very thin and created the appearance of a thickened postsynaptic membrane, rather than forming a discrete thickening below the postsynaptic membrane.

Postsynaptic profiles were identified as perikarya, larger caliber (>1 μm) and smaller caliber (<1 μm) dendrites, and dendritic spines by using established morphological criteria (Peters et al., 1991). Although CaMK immunoreactivity is a reliable marker for perikarya and dendrites of BLa pyramidal cells, many spines of pyramidal cells do not exhibit CaMK immunoreactivity (McDonald et al., 2002). However, because the results of previous studies suggest that the great majority of spines seen in electron microscopic studies belong to pyramidal cells (for discussion see Muller et al., 2006), all spines, whether CaMK$^+$ or not, were considered to be of pyramidal cell origin.

For both CaMK and PV preparations, the frequency of synaptic contacts from VAChT$^+$ terminals, and the identification of their postsynaptic targets, was tallied and pooled from the two brains judged to have the best ultrastructural preservation and immunohistochemistry for both VAChT and the neuronal markers. To get sufficient sampling of all cellular compartments, it was necessary for the samples to meet these criteria for large, continuous areas. Labeled terminals were partially reconstructed from serial sections (four to six serial sections per terminal). In VAChT/CaMK and VAChT/PV preparations, both labeled and unlabeled synaptic targets of VAChT$^+$ terminals were counted.

Antibody specifity

The VAChT antibody was raised in goat by using a synthetic carboxy-terminal 20-amino-acid sequence (511–530) from the cloned rat VAChT as an immunogen and has previously been characterized (Arvidsson et al., 1997). The antiserum immunohistochemically stains CV-1 cells transfected with rat VAChT cDNA but not vesicular monoamine transporter-2 (VMAT-2) cDNA (Arvidsson et al., 1997). VAChT immunoreactivity was also seen in cells that are known to express the protein, such as PC12 cells and cultured spinal motoneurons. Preadsorption of the antiserum with the immunizing peptide completely abolished immunostaining (Arvidsson et al., 1997).

The polyclonal PV antiserum (antiserum R-301; generously donated by Dr. Kenneth Baimbridge, University of British Columbia) was raised in rabbit against rat muscle PV. Previous studies have shown that immunohistochemical staining with this antiserum was blocked by preadsorption of the antiserum with PV, but not calretinin or calbindin (Conde et al., 1994).

The mouse monoclonal antibody to the α-subunit of CaMK (Sigma; catalog No. C265; clone 6G9) was raised against purified type II CaMK. This antibody binds with high affinity to purified α-subunit of CaMK obtained from rat brain on immunoblots and produces a single line at 50 kDa (Kennedy et al., 1983). It also recognizes a single protein band at 50 kDa on immunoblots of rat brain homogenates (Erondu and Kennedy, 1985). Additional immunoblot studies revealed that the antibody recognizes both phosphorylated and nonphosphorylated forms of the kinase (Erondu and Kennedy, 1985).

Author Manuscript Author Manuscript Author Manuscript Author Manuscript

RESULTS

Light microscopic examination revealed that the BLC contained a plexus of thin VAChT$^+$ axons, which varied in density in the various nuclei of the complex. The density of this axonal plexus was greatest in the BLa and BLp (anterior and posterior subdivisions of the basolateral nucleus) and significantly less in the lateral and basomedial nuclei (Fig. 1A,C,D). Within the basolateral nucleus, the density of the axonal plexus was greater in more anterior portions of the nucleus (Fig. 1). Axonal morphology was similar in all portions of the BLC. Axonal varicosities were very small (~0.5 μm), and intervaricose segments of VAChT$^+$ axons were either unstained or very lightly stained (Fig. 1B). Occasional VAChT$^+$ cell bodies were observed along the medial and ventral borders of the BLa at rostral levels. The morphology of these cells closely resembled that of the large VAChT$^+$ cholinergic neurons seen in the overlying striatum. No small VAChT$^+$ neurons resembling the choline acetyltransferase-positive (ChAT$^+$) bipolar interneurons described in previous studies (Carlsen and Heimer, 1986; see also Nitecka and Frotscher, 1989, and Li et al., 2001) were observed, even in the animals that received colchicine injections.

In the electron microscope, VAChT$^+$ terminals were approximately 0.5 μm in cross-sectional diameter, although some subtle swellings were smaller and some terminals appeared larger in oblique or longitudinal view (Figs. 2–7). The DAB reaction product was diffuse throughout the terminal, darkest around the synaptic vesicle membranes, and relatively light or clear in the lumens of synaptic vesicles (Figs. 2–7). Synaptic vesicles in VAChT$^+$ terminals were round, medium-sized, and fairly uniform; dense-core vesicles were rarely seen. Even in a short series of thin sections, the majority of VAChT$^+$ terminals made synaptic contacts, and virtually all of these synapses were symmetrical. Although most VAChT$^+$ terminals were separated from each another, it was not uncommon to see VAChT$^+$ profiles adjacent to one another (Figs. 3, 4) and in some cases clustered around the same dendrite (Fig. 4B).

The granular V-VIP reaction product in postsynaptic pyramidal cell profiles (CaMK$^+$) and PV$^+$ interneuronal profiles was easily distinguished from the dense, diffuse DAB reaction product in VAChT$^+$ terminals. The innervation of CaMK$^+$ pyramidal cells by VAChT$^+$ terminals included all major cellular compartments: perikarya (Fig. 2), large- and small-caliber dendrites (Figs. 3, 4), and spines (Figs. 3, 5). From initial qualitative surveys, it was clear that small-caliber CaMK$^+$ dendritic shafts were the predominant targets, with many dendritic segments receiving multiple synaptic inputs (Figs. 3, 4). The quantitative survey was sampled from two different animals where the VAChT and CaMK$^+$ immunoreactivity and overall morphology were superior, yielding similar results (Table 2). The main targets in each animal were small-caliber CaMK$^+$ dendritic shafts and spines. In the pooled results for the two animals, among 152 synapses from VAChT$^+$ terminals, 136 (89.5%) of the targets were of pyramidal cell origin (i.e., either CaMK-positive structures or dendritic spines), and the remaining 16 (10.5%) were unlabeled dendrites. Pyramidal cell small-caliber dendrites (62; 40.8%) and spines (60; 39.5%) made up a total of 80.3% of the postsynaptic targets.

Initial surveys of preparations labeled for VAChT and parvalbumin (PV) immunoreactivity found VAChT$^+$ terminals making synaptic contact onto the perikarya of PV$^+$ interneurons

Author Manuscript Author Manuscript Author Manuscript Author Manuscript

(Fig. 6) as well as large- and small-caliber PV^+ dendrites (Fig. 7). Quantitative surveys from two different animals, in which the $VAChT^+$ and PV^+ immunoreactivity and overall morphology were superior over a large area of the section, yielded similar results (Table 3). The pooled results showed that, among 177 synapses counted, 12 (6.8%) were onto PV^+ dendrites, 10 of which were less than 1 μm in diameter. In these preparations, the primary targets overall were unlabeled small-caliber dendrites (42.4%) and spines (38.4%).

In addition to instances in which $VAChT^+$ terminals were clustered around the same dendrite (Fig. 4B), $VAChT^+$ terminals were often adjacent to or in close proximity to other terminals synapsing onto the same profile. This arrangement was particularly notable on dendritic spines (Figs. 3, 5) and among asymmetric (excitatory) synaptic inputs to PV^+ dendrites (Fig. 7).

DISCUSSION

This is the first study to quantify the distribution of cholinergic synaptic inputs onto defined neuronal populations in the basolateral amygdala. This was made possible, in part, by using antibodies to CaMK to label selectively cell bodies and dendritic shafts of pyramidal cells. Most cholinergic terminals, as characterized by VAChT immunoreactivity, were small, were packed with round vesicles of uniform size, and formed symmetrical synapses. Their main targets in the BLa were small-caliber (distal) dendrites and spines of pyramidal cells, with many dendritic segments receiving multiple synaptic contacts. Interneurons immunoreactive for parvalbumin (PV^+) also received significant innervation, mainly on their dendrites.

Cholinergic structures and synapses in the BLC

Previous light microscopic studies of the distribution of VAChT-positive cholinergic structures in the rat brain have noted that the BLC receives a dense innervation by $VAChT^+$ axons that matches the high density of choline acetyltransferase-positive ($ChAT^+$) axons in this brain region (Gilmor et al., 1996; Ichikawa et al., 1997; Arviddson et al., 1997; Schäfer et al., 1998). This similarity is not surprising, insofar as both proteins are produced from a common “cholinergic operon” (Usdin et al., 1995; Weihe et al., 1996). In situ hybridization and immunohistochemical studies have demonstrated that neurons expressing ChAT and VAChT exhibit very similar distribution patterns throughout the brain, and these markers, and their mRNAs, have been found to colocalize extensively (Gilmor et al., 1996; Arvidsson et al., 1997; Ichikawa et al., 1997). In fact, VAChT has been found to be a stronger marker for cholinergic terminals than ChAT (Gilmor et al., 1996; Weihe et al., 1996). The morphology of $VAChT^+$ axons in our investigation, at both the light and the electron microscopic levels of analysis, appeared to be identical to that described in previous studies of the BLa using ChAT antibodies as cholinergic markers (Wainer et al., 1984; Carlsen and Heimer, 1986; Nitecka and Frotscher, 1989; Houser, 1990; Li et al., 2001).

Some immunohistochemical studies have reported the existence of a small number of $ChAT^+$ bipolar interneurons in the BLC (~5 per 50-μm-thick section through the BLa, Carlsen and Heimer, 1986; see also Nitecka and Frotscher, 1989, and Li et al., 2001), similarly to the cerebral cortex (Houser et al., 1985). The staining of these neurons with two different monoclonal antibodies that recognize different epitopes suggests that this staining

Author Manuscript Author Manuscript Author Manuscript Author Manuscript

is not due to recognition of an unrelated protein. As in previous VAChT immunohistochemical studies that have commented on the amygdala (Gilmor et al., 1996; Ichikawa et al., 1997; Arvidsson et al., 1997), no VAChT$^+$ interneurons were observed in the BLC in the present investigation, despite strong staining of the perikarya of striatal and basal forebrain cholinergic neurons. Even the injection of colchicine, which interrupts the transport of proteins from the cell body to axon terminals by disrupting microtubules, failed to generate VAChT immunoreactivity in small bipolar interneurons in the BLC in the present study. Although this suggests that cholinergic bipolar interneurons in the BLC do not express VAChT, it is possible that the perikaryal levels of VAChT are below the level needed for immunodetection, perhaps as a result of very slow turnover of VAChT in these neurons. If this is the case, then some of the VAChT$^+$ axon terminals seen in the present study may be associated with axons of cholinergic interneurons whose perikarya do not have detectable levels of VAChT. Bipolar cholinergic interneurons in the cortex have very modest axonal arborizations (von Engelhardt et al., 2007), as do Golgi-stained bipolar/bitufted interneurons in the BLC (McDonald, 1982). Thus, even if the axon terminals of the few cholinergic inter-neurons in the BLC are VAChT$^+$, it is unlikely that many were observed in our sample. This conclusion is also supported by the uniform morphology of VAChT$^+$ terminals seen in the present study. It is therefore presumed that the great majority (or perhaps all) of the VAChT$^+$ axon terminals observed in the present study originate from cholinergic neurons of the basal forebrain.

In the present study, the majority of VAChT$^+$ terminals examined formed synaptic contacts, even though complete serial-section reconstructions of each terminal were not performed. Virtually all of these synapses were symmetrical. These findings agree with previous ultrastructural studies of ChAT$^+$ axon terminals in the BLa (Wainer et al., 1984; Carlsen and Heimer, 1986; Nitecka and Frotscher, 1989; Houser, 1990; Li et al., 2001) and suggest that conventional synaptic release is the primary mode of cholinergic transmission in the BLa.

Innervation of BLa pyramidal cells by cholinergic terminals

Previous ultrastructural studies of the cholinergic innervation of the BLa using ChAT as a marker found labeled terminals making synaptic contacts mainly with dendritic shafts and, to a lesser extent, with dendritic spines (Wainer et al., 1984; Carlsen and Heimer, 1986; Houser, 1990; Li et al., 2001), although none of these studies used quantitative methods to determine the exact ratio of these postsynaptic targets. As in the present study, these synapses were generally symmetrical, although some asymmetrical synapses with spines were also described. Although most of the spines probably belonged to pyramidal cells, the cells of origin of the dendritic shafts could not be determined in these single-label ChAT studies. The use of CaMK antibodies to label pyramidal cell dendrites selectively in the present study, in conjunction with counts of postsynaptic targets, allowed us to determine that the great majority (82%; 72/88) of the dendritic shafts receiving VAChT$^+$ synapses belonged to pyramidal cells. If all spines (both CaMK-positive and CaMK-negative) are considered to be of pyramidal cell origin, then the total percentage of VAChT$^+$ terminals forming synapses with pyramidal cells is 89% (136/152). Moreover, 90% (122/136) of the pyramidal cell targets, and 80% (122/152) of the total targets of VAChT$^+$ terminals, were small-caliber distal dendrites and spines of BLa pyramidal cells. Thus, the synaptic

Author Manuscript Author Manuscript Author Manuscript Author Manuscript

modulation of the BLa by cholinergic afferents from the basal forebrain would appear to be mediated primarily by inputs to the distal dendritic compartment of pyramidal cells.

These findings are consistent with electrophysiological studies that have demonstrated that cholinergic transmission in the basolateral amygdala increases the excitability of pyramidal cells via both nicotinic receptors (Klein and Yakel, 2006) and muscarinic receptors (Washburn and Moises, 1992; Womble and Moises, 1992, 1993; Yajeya et al., 1997, 1999; Power and Sah, 2008; Power et al., 2008). Postsynaptic cholinergic activation of nicotinic receptors on BL pyramidal cell perikarya and dendrites is characterized by rapid activation kinetics and pharmacological selectivity for receptors containing α7 subunits (Klein and Yakel, 2006). One of the main effects of muscarinic agonists and/or stimulation of cholinergic afferents to the amygdala is an increase in the excitability of BLC pyramidal cells resulting from the suppression of several potassium currents, including the muscarine sensitive M-current (I_M), a voltage-insensitive leak current (I_{Leak}), a hyperpolarization-activated inward rectifier current (I_Q), and the calcium-activated slow afterhyperpolarization current (sI_{AHP}; Washburn and Moises, 1992; Womble and Moises, 1992, 1993; Yajeya et al., 1999; Power and Sah, 2008; Power et al., 2008). Electrophysiological studies indicate that most sI_{AHP} channels are located along distal dendrites of BLC pyramidal neurons (Power and Sah, 2008; Power et al., 2008), which correlates with the largely dendritic distribution of cholinergic synaptic inputs to these neurons seen in the present study. Interestingly, there is evidence that the cholinergic suppression of sI_{AHP} channels in hippocampal pyramidal cells is mediated by activation of CaMK (Muller et al., 1992), the marker used in the present study to identify the dendritic shafts of BLC pyramidal neurons. For the BLC, it is thought that suppression of sI_{AHP} channels not only attenuates spike frequency adaptation but also is involved in the modulation of synaptic inputs to pyramidal cells (Power et al., 2008). Finally, a recent study has demonstrated that activation of muscarinic cholinergic receptors activates small-conductance calcium-activated potassium (SK) channels in BLC pyramidal cells, following the release of calcium from intracellular stores via activation of the phosphatidylinositol signal transduction pathway (Power and Sah, 2008). Because the M1 family of cholinergic receptors is known to activate the phosphatidylinositol system (Richelson, 1995), M1 receptors in BLC pyramidal cells may mediate this response. This is consistent with strong M1 receptor immunoreactivity in BLC pyramidal cells (McDonald and Mascagni, 2010).

Innervation of BLa interneurons by cholinergic terminals

The results of our VAChT/CaMK analysis revealed that about 10% of $VAChT^+$ terminals in the BLa formed synapses with CaMK-negative dendrites, presumed to be dendrites of GABAergic interneurons. Our VAChT/PV studies suggest that more than half of these dendrites belong to the PV^+ subpopulation of GABAergic interneurons (6.8% of all structures postsynaptic to $VAChT^+$ terminals). Moreover, our qualitative survey found synaptic contacts with PV^+ perikarya as well. Because interneurons constitute about 15% of the total neuronal population in the BLa (McDonald, 1992b), and PV^+ neurons constitute about 40% of all interneurons in the BLa (Mascagni and McDonald, 2003), the percentage of PV^+ interneurons targeted by cholinergic terminals is proportional to their occurrence in

Author Manuscript Author Manuscript Author Manuscript Author Manuscript

this nucleus (about 6%). Interestingly, the same is true for pyramidal cells (85% of the total neuronal population in the BLa; 89% of the targets of cholinergic terminals).

These results regarding interneurons are consistent with previous nonquantitative ultrastructural analyses of cholinergic afferents to the BLa (Carlsen and Heimer, 1986; Nitecka and Frotscher, 1989). Thus, Carlsen and Heimer (1986) observed $ChAT^+$ terminals forming synapses with perikarya of unlabeled interneurons identified using morphological criteria. They also found occasional $ChAT^+$ synapses with $ChAT^+$ interneuronal perikarya. Nitecka and Frotscher (1989) reported that $ChAT^+$ terminals formed contacts, including synapses, with GAD^+ interneuronal cell bodies and dendrites. Both muscarinic (Washburn and Moises, 1992; Yajeya et al., 1997) and nicotinic (Zhu et al., 2005) agonists have been found to increase the excitability of fast-spiking GABAergic interneurons in the BLa. An indirect effect of muscarinic excitation of fast-spiking GABAergic interneurons (Washburn and Moises, 1992) was seen as a rapid-onset, early hyperpolarization in pyramidal cells, followed by prolonged depolarization, the direct muscarinic effect on the pyramidal cells (Washburn and Moises, 1992). Insofar as most fast-spiking interneurons in the BLa have been found to be PV^+ (Rainnie et al., 2006; Woodruff and Sah, 2007a), our finding that PV^+ interneurons receive direct synaptic input from $VAChT^+$ terminals is consistent with the cholinergic physiological data. In whole-cell recordings in the BLa, nicotinic activation of GABAergic interneurons elicited an increase in spontaneous inhibitory postsynaptic currents (sIPSCs) in pyramidal cells (Zhu et al., 2005). This effect was selectively blocked by an antagonist specific for the $\alpha 3\beta 4$ subunit combination, evidence that nicotinic postsynaptic effects on interneurons and pyramidal cells in the basolateral amygdala are distinguishable by their receptors' subunit composition (see above).

Anatomical associations of cholinergic and noncholinergic terminals

$VAChT^+$ terminals in close proximity to unlabeled terminals forming symmetrical (usually inhibitory) synapses and to unlabeled or CaMK-labeled terminals forming asymmetrical (presumed excitatory) synapses were observed in the present study. These associations were most obvious on some spines of pyramidal neurons (see, e.g., Figs. 3, 5) and on dendrites of PV^+ interneurons (see, e.g., Fig. 7). Postsynaptic interactions of these inputs might allow cholinergic synapses to modulate the postsynaptic responses of glutamatergic or GABAergic inputs to BLC neurons (or vice versa). If the noncholinergic terminals express cholinergic receptors, it is also possible that synaptic spillover of acetylcholine during high rates or bursts of cholinergic activity could modulate the release of glutamate or GABA from these terminals (or vice versa; Vizi and Kiss, 1998; Sarter et al., 2009). In a previous paper, Li and coworkers (2001) reported that $ChAT^+$ axon terminals in the BLa formed synaptic junctions with adjacent axon terminals. In the present study, no clear examples of cholinergic axoaxonal synapses were found.

These findings are consistent with electrophysiological studies of the BLC that have demonstrated modulation of glutamate and GABA release from axon terminals by cholinergic mechanisms. In general, presynaptic muscarinic receptors inhibit release from glutamatergic and GABAergic terminals, whereas presynaptic nicotinic receptors increase release. In the lateral nucleus of the BLC, muscarinic suppression of GABAergic and

Author Manuscript Author Manuscript Author Manuscript Author Manuscript

glutamatergic release was found to be receptor subtype specific, mediated by M1 and M3 muscarinic receptors, respectively (Sugita et al., 1991). In another study, muscarinic suppression of glutamatergic release from cortical terminals in the BLC was found to involve multiple muscarinic receptor subtypes (Yajeya et al., 2000). There is also evidence for differential reduction of inhibitory transmission in different subpopulations of GABAergic interneurons via M2 muscarinic receptors in the BLC (Szabo et al., 2009). Nicotinic enhancement of glutamatergic and GABAergic release in the BLC has been found to be receptor subtype specific as well, with glutamatergic cortical afferents expressing nicotinic receptors composed of α7 and α4/β2 subunits (Jiang and Role, 2008) and GABAergic terminals containing nicotinic receptors composed of α3/β4 subunits (Zhu et al., 2005). Thus the specific distribution of muscarinic and nicotinic receptors among GABAergic and glutamatergic terminals can determine the weighting of various synaptic pathways, in response to the dynamics of cholinergic transmission. Future immunocytochemical studies involving dual labeling of cholinergic terminals and cholinergic receptors at the ultrastructural level are needed to help clarify these issues in the BLC.

Functional implications

Cholinergic neurotransmission in the BLC plays an important role in mnemonic function and long-term potentiation (Power et al., 2003; Paré, 2003; Jiang and Role, 2008; Huang et al., 2008). The main function associated with the cholinergic innervation of the BLC is memory consolidation in a wide variety of learning tasks (for review see Power et al., 2003). It is thought that the BLC enhances memory consolidation by promoting interactions between hippocampal regions and neocortical memory storage sites (Paré, 2003). These interactions appear to depend on the generation of synchronous theta oscillations among these structures, which create recurring time windows that facilitate synaptic interactions and promote synaptic plasticity (Pelletier and Paré, 2004; Pape and Paré, 2010). The results of anatomical and electrophysiological studies suggest that the innervation of BLC pyramidal neurons and PV^+ interneurons by basal forebrain cholinergic inputs may play a major role in generating these oscillations.

Thus, in addition to projections to extrinsic regions such as the hippocampal region and cerebral cortex, BLC pyramidal cells have extensive local axonal arborizations (Pitkänen et al., 2003; McDonald et al., 2005) that provide a dense innervation of the dendritic spines of numerous surrounding pyramidal cells, which could promote synchronous firing of these cells (Paré and Gaudreau, 1996; Smith et al., 2000). BLC pyramidal cells also have a largely perisomatic innervation of neighboring PV^+ inter-neurons, which can provide potent excitation of these neurons (Morys et al., 1999; Smith et al., 2000; McDonald et al., 2005; Woodruff and Sah, 2007b). It has been shown that activation of a network of PV^+ basket cells in the hippocampus, interconnected by dendritic gap junctions and GABAergic chemical synapses, plays an important role in the generation and maintenance of oscillatory activity in this brain region (Freund and Buzsaki, 1996; Freund, 2003). Recent studies have shown that similar networks of PV^+ neurons also exist in the BLC (Muller et al., 2005; Woodruff and Sah, 2007a) and that these networks can entrain the firing of a large number of neighboring pyramidal cells via a robust, inhibitory, perisomatic innervation (Rainnie et

Author Manuscript Author Manuscript Author Manuscript Author Manuscript

al., 2006; Woodruff and Sah, 2007a,b). The existence of reciprocal interconnections between excitatory pyramidal cells and inhibitory PV^+ interneurons is consistent with electrophysiological studies in the BLC that have demonstrated counterphase firing of pyramidal cells and fast-firing (presumptive PV^+) interneurons during theta rhythms (Paré and Gaudreau, 1996).

As discussed above, electrophysiological studies indicate that the robust cholinergic innervation of pyramidal cells and PV^+ interneurons observed in the present study is associated with excitation of both types of neurons by muscarinic and nicotinic receptors. Given the anatomy and physiology of the reciprocal interconnections between these neurons, rhythmic oscillations are likely to be produced by this activation. Moreover, BLC pyramidal cells have intrinsic conductances, including conductances sensitive to muscarinic cholinergic agonists, that produce theta (Paré et al., 1995; Pape et al., 1998). It has been suggested that muscarinic cholinergic reduction of the slow AHP current may facilitate these theta oscillations in BLC pyramidal cells (Pape et al., 2005). If the amygdala is like the hippocampus, nicotinic influences may not be critical for generating oscillations but may be important for modulating preexisting oscillatory states (Cobb and Davies, 2005). In addition, recent studies indicate that corticopetal cholinergic neurons in the basal forebrain fire at theta frequency (Lee et al., 2005). If amygdalopetal cholinergic basal forebrain neurons have similar firing patterns, this would also promote the generation of theta rhythms in the BLC.

Acknowledgments

Grant sponsor: National Institutes of Health; Grant number: R01-DA027305.

The authors are grateful to Dr. Kenneth Baimbridge (University of British Columbia) for the donation of the rabbit polyclonal antibody to PV.

LITERATURE CITED

Amaral DG, Bassett JL. Cholinergic innervation of the monkey amygdala: an immunohistochemical analysis with antisera to choline acetyltransferase. J Comp Neurol. 1989; 281:337–361. [PubMed: 2703552]

Arvidsson U, Riedl M, Elde R, Meister B. Vesicular acetylcholine transporter (VAChT) protein: a novel and unique marker for cholinergic neurons in the central and peripheral nervous systems. J Comp Neurol. 1997; 378:454–467. [PubMed: 9034903]

Carlsen J, Heimer L. A correlated light and electron microscopic immunocytochemical study of cholinergic terminals and neurons in the rat amygdaloid body with special emphasis on the basolateral amygdaloid nucleus. J Comp Neurol. 1986; 244:121–136. [PubMed: 3512630]

Carlsen J, Heimer L. The basolateral amygdaloid complex as a cortical-like structure. Brain Res. 1988; 441:377–380. [PubMed: 2451985]

Carlsen J, Zaborszky L, Heimer L. Cholinergic projections from the basal forebrain to the basolateral amygdaloid complex: a combined retrograde fluorescent and immunohistochemical study. J Comp Neurol. 1985; 234:155–167. [PubMed: 3886715]

Cobb SR, Davies CH. Cholinergic modulation of hippocampal cells and circuits. J Physiol. 2005; 562:81–88. [PubMed: 15528238]

Conde F, Lund JS, Jacobowitz DM, Baimbridge KG, Lewis DA. Local circuit neurons immunoreactive for calretinin, calbindin D-28k or parvalbumin in monkey prefrontal cortex: distribution and morphology. J Comp Neurol. 1994; 341:95–116. [PubMed: 8006226]

Author Manuscript Author Manuscript Author Manuscript Author Manuscript

Emre M, Heckers S, Mash DC, Geula C, Mesulam MM. Cholinergic innervation of the amygdaloid complex in the human brain and its alterations in old age and Alzheimer's disease. J Comp Neurol. 1993; 336:117–134. [PubMed: 8254109]

Erondu NE, Kennedy MB. Regional distribution of type II Ca2/calmodulin-dependent protein kinase in rat brain. J Neurosci. 1985; 5:3270–3277. [PubMed: 4078628]

Freund TF. Interneuron Diversity Series: rhythm and mood in perisomatic inhibition. Trends Neurosci. 2003; 26:489–495. [PubMed: 12948660]

Freund TF, Buzsáki G. Interneurons of the hippocampus. Hippocampus. 1996; 6:347–470. [PubMed: 8915675]

Gilmor ML, Nash NR, Roghani A, Edwards RH, Yi H, Hersch SM, Levey AI. Expression of the putative vesicular acetylcholine transporter in rat brain and localization in cholinergic synaptic vesicles. J Neurosci. 1996; 16:2179–2190. [PubMed: 8601799]

Hancock MB. Two color immunoperoxidase staining: visualization of anatomic relationships between immunoreactive neural elements. Am J Anat. 1986; 175:343–352. [PubMed: 2422916]

Houser CR. Cholinergic synapses in the central nervous system: studies of the immunocytochemical localization of choline acetyltransferase. J Elec Microsc Techniq. 1990; 15:2–19.

Houser CR, Crawford GD, Salvaterra PM, Vaughn JE. Immunocytochemical localization of choline acetyltransferase in rat cerebral cortex: a study of cholinergic neurons and synapses. J Comp Neurol. 1985; 234:17–34. [PubMed: 3980786]

Huang YY, Kandel ER, Levine A. Chronic nicotine exposure induces a long-lasting and pathway-specific facilitation of LTP in the amygdala. Learn Mem. 2008; 15:603–610. [PubMed: 18685152]

Ichikawa T, Ajiki K, Matsuura J, Misawa H. Localization of two cholinergic markers, choline acetyltransferase and vesicular acetylcholine transporter in the central nervous system of the rat: in situ hybridization histochemistry and immunohistochemistry. J Chem Neuroanat. 1997; 13:23–39. [PubMed: 9271193]

Jiang L, Role LW. Facilitation of cortico-amygdala synapses by nicotine: activity-dependent modulation of glutamatergic transmission. J Neurophysiol. 2008; 99:1988–1999. [PubMed: 18272879]

Kemppainen S, Pitkänen A. Distribution of parvalbumin, calretinin, and calbindin-D(28k) immunoreactivity in the rat amygdaloid complex and colocalization with gamma-aminobutyric acid. J Comp Neurol. 2000; 426:441–467. [PubMed: 10992249]

Kennedy MB, Bennett MK, Erondu NE. Biochemical and immunochemical evidence that the "major postsynaptic density protein" is a subunit of a calmodulin-dependent protein kinase. Proc Natl Acad Sci U S A. 1983; 80:7357–7361. [PubMed: 6580651]

Klein RC, Yakel JL. Functional somatodendritic alpha7-containing nicotinic acetylcholine receptors in the rat basolateral amygdala complex. J Physiol. 2006; 576:865–872. [PubMed: 16931547]

Kordower JH, Bartus RT, Marciano FF, Gash DM. Telencephalic cholinergic system of the New World monkey (*Cebus apella*): morphological and cytoarchitectonic assessment and analysis of the projection to the amygdala. J Comp Neurol. 1989; 279:528–545. [PubMed: 2465322]

Lanciego JL, Goede PH, Witter MP, Wouterlood FG. Use of peroxidase substrate Vector VIP for multiple staining in light microscopy. J Neurosci Methods. 1997; 74:1–7. [PubMed: 9210569]

Lee MG, Hassani OK, Alonso A, Jones BE. Cholinergic basal forebrain neurons burst with theta during waking and paradoxical sleep. J Neurosci. 2005; 25:4365–4369. [PubMed: 15858062]

Li R, Nishijo H, Wang Q, Uwano T, Tamura R, Ohtani O, Ono T. Light and electron microscopic study of cholinergic and noradrenergic elements in the basolateral nucleus of the rat amygdala: evidence for interactions between the two systems. J Comp Neurol. 2001; 439:411–425. [PubMed: 11596063]

Mascagni F, McDonald AJ. Immunohistochemical characterization of cholecystokinin containing neurons in the rat basolateral amygdala. Brain Res. 2003; 976:171–184. [PubMed: 12763251]

McDonald AJ. Neurons of the lateral and basolateral amygdaloid nuclei: a Golgi study in the rat. J Comp Neurol. 1982; 212:293–312. [PubMed: 6185547]

McDonald AJ. Neuronal organization of the lateral and basolateral amygdaloid nuclei in the rat. J Comp Neurol. 1984; 222:589–606. [PubMed: 6199387]

Author Manuscript Author Manuscript Author Manuscript Author Manuscript

McDonald, AJ. Cell types and intrinsic connections of the amygdala. In: Aggleton, JP., editor. The amygdala. New York: Wiley-Liss; 1992a. p. 67-96.

McDonald AJ. Projection neurons of the basolateral amygdala: a correlative Golgi and retrograde tract tracing study. Brain Res Bull. 1992b; 28:179–185. [PubMed: 1375860]

McDonald AJ, Betette R. Parvalbumin containing neurons in the rat basolateral amygdala: morphology and colocalization of calbindin D-28k. Neuroscience. 2001; 102:413–425. [PubMed: 11166127]

McDonald AJ, Mascagni F. Colocalization of calcium-binding proteins and gamma-aminobutyric acid in neurons of the rat basolateral amygdala. Neuroscience. 2001; 105:681–693. [PubMed: 11516833]

McDonald AJ, Mascagni F. Immunohistochemical characterization of somatostatin containing interneurons in the rat basolateral amygdala. Brain Res. 2002; 943:237–244. [PubMed: 12101046]

McDonald AJ, Mascagni F. Neuronal localization of m1 muscarinic receptor immunoreactivity in the rat basolateral amygdala. Brain Struct Funct. 2010; 215:37–48. [PubMed: 20503057]

McDonald AJ, Muller JF, Mascagni F. GABAergic Innervation of alpha type II calcium/calmodulin-dependent protein kinase immunoreactive pyramidal neurons in the rat basolateral amygdala. J Comp Neurol. 2002; 446:199–218. [PubMed: 11932937]

McDonald AJ, Mascagni F, Mania I, Rainnie DG. Evidence for a perisomatic innervation of parvalbumin-containing interneurons by individual pyramidal cells in the basolateral amygdala. Brain Res. 2005; 1035:32–40. [PubMed: 15713274]

McGaugh JL. The amygdala modulates the consolidation of memories of emotionally arousing experiences. Annu Rev Neurosci. 2004; 27:1–28. [PubMed: 15217324]

McIntyre CK, Ragozzino ME, Gold PE. Intra-amygdala infusions of scopolamine impair performance on a conditioned place preference task but not a spatial radial maze task. Behav Brain Res. 1998; 95:219–226. [PubMed: 9806441]

Mesulam MM, Mufson EJ, Wainer BH, Levey AI. Central cholinergic pathways in the rat: an overview based on an alternative nomenclature (Ch1–Ch6). Neuroscience. 1983a; 10:1185–1201. [PubMed: 6320048]

Mesulam MM, Mufson EJ, Levey AI, Wainer BH. Cholinergic innervation of cortex by the basal forebrain: cytochemistry and cortical connections of the septal area, diagonal band nuclei, nucleus basalis (substantia innominata), and hypothalamus in the rhesus monkey. J Comp Neurol. 1983b; 214:170–197. [PubMed: 6841683]

Moryś J, Berdel B, Kowiaski P, Majak K, Tarnawski M, Wisniewski HM. Relationship of calcium-binding protein containing neurons and projection neurons in the rat basolateral amygdala. Neurosci Lett. 1999; 259:91–94. [PubMed: 10025565]

Muller JF, Mascagni F, McDonald AJ. Coupled networks of parvalbumin-immunoreactive interneurons in the rat basolateral amygdala. J Neurosci. 2005; 25:7366–7376. [PubMed: 16093387]

Muller JF, Mascagni F, McDonald AJ. Pyramidal cells of the rat basolateral amygdala: synaptology and innervation by parvalbumin-immunoreactive interneurons. J Comp Neurol. 2006; 494:635–650. [PubMed: 16374802]

Muller JF, Mascagni F, McDonald AJ. Serotonin-immunoreactive axon terminals innervate pyramidal cells and inter-neurons in the rat basolateral amygdala. J Comp Neurol. 2007; 505:314–335. [PubMed: 17879281]

Muller W, Petrozzino JJ, Griffith LC, Danho W, Connor JA. Specific involvement of Ca^{2+}-calmodulin kinase II in cholinergic modulation of neuronal responsiveness. J Neurophysiol. 1992; 68:2264–2269. [PubMed: 1337106]

Nitecka L, Frotscher M. Organization and synaptic interconnections of GABAergic and cholinergic elements in the rat amygdaloid nuclei: single- and double-immunolabeling studies. J Comp Neurol. 1989; 279:470–488. [PubMed: 2918082]

Pape HC, Paré D. Plastic synaptic networks of the amygdala for the acquisition, expression, and extinction of conditioned fear. Physiol Rev. 2010; 90:419–463. [PubMed: 20393190]

Pape HC, Paré D, Driesang RB. Two types of intrinsic oscillations in neurons of the lateral and basolateral nuclei of the amygdala. J Neurophysiol. 1998; 79:205–216. [PubMed: 9425192]

Author Manuscript Author Manuscript Author Manuscript Author Manuscript

Pape HC, Narayanan RT, Smid J, Stork O, Seidenbecher T. Theta activity in neurons and networks of the amygdala related to long-term fear memory. Hippocampus. 2005; 15:874–880. [PubMed: 16158424]

Paré D. Role of the basolateral amygdala in memory consolidation. Prog Neurobiol. 2003; 70:409–420. [PubMed: 14511699]

Paré D, Gaudreau H. Projection cells and interneurons of the lateral and basolateral amygdala: distinct firing patterns and differential relation to theta and delta rhythms in conscious cats. J Neurosci. 1996; 16:3334–3350. [PubMed: 8627370]

Paré D, Pape HC, Dong J. Bursting and oscillating neurons of the cat basolateral amygdaloid complex in vivo: electrophysiological properties and morphological features. J Neurophysiol. 1995; 74:1179–1191. [PubMed: 7500142]

Paxinos, G.; Watson, C. The rat brain in stereotaxic coordinates. New York: Academic Press; 1997.

Pelletier JG, Paré D. Role of amygdala oscillations in the consolidation of emotional memories. Biol Psychiatry. 2004; 55:559–562. [PubMed: 15013823]

Peters, A.; Palay, SL.; Webster, HD. The fine structure of the nervous system. New York: Oxford University Press; 1991.

Pitkänen A, Savander M, Nurminen N, Ylinen A. Intrinsic synaptic circuitry of the amygdala. Ann N Y Acad Sci. 2003; 985:34–49. [PubMed: 12724146]

Power AE, Vazdarjanova A, McGaugh JL. Muscarinic cholinergic influences in memory consolidation. Neurobiol Learn Mem. 2003; 80:178–193. [PubMed: 14521862]

Power JM, Sah P. Competition between calcium-activated K^+ channels determines cholinergic action on firing properties of basolateral amygdala projection neurons. J Neurosci. 2008; 28:3209–3220. [PubMed: 18354024]

Power, JM.; Bocklisch, S.; Sah, P. Program No. 44.24, 2008 Neuroscience meeting planner. Washington, DC: Society for Neuroscience; 2008. Localization and function of the sIAHP in basolateral amygdalar projection neurons. Online

Rainnie DG, Asprodini EK, Shinnick-Gallagher P. Intracellular recordings from morphologically identified neurons of the basolateral amygdala. J Neurophysiol. 1993; 69:1350–1361. [PubMed: 8492168]

Rainnie DG, Mania I, Mascagni F, McDonald AJ. Physiological and morphological characterization of parvalbumin-containing interneurons of the rat basolateral amygdala. J Comp Neurol. 2006; 498:142–161. [PubMed: 16856165]

Richelson, E. Cholinergic transduction. In: Bloom, FE.; Kupfer, DJ., editors. Psychopharmacology: the fourth generation of progress. New York: Raven Press; 1995. p. 25-134.

Sah P, Faber ES, Lopez De Armentia M, Power J. The amygdaloid complex: anatomy and physiology. Physiol Rev. 2003; 83:803–834. [PubMed: 12843409]

Salinas JA, Introini-Collison IB, Dalmaz C, McGaugh JL. Posttraining intraamygdala infusions of oxotremorine and propranolol modulate storage of memory for reductions in reward magnitude. Neurobiol Learn Mem. 1997; 68:51–59. [PubMed: 9195589]

Sarter M, Parikh V, Howe WM. Phasic acetylcholine release and the volume transmission hypothesis: time to move on. Nat Rev Neurosci. 2009; 10:383–390. [PubMed: 19377503]

Schäfer MK, Eiden LE, Weihe E. Cholinergic neurons and terminal fields revealed by immunohistochemistry for the vesicular acetylcholine transporter. I. Central nervous system. Neuroscience. 1998; 84:331–359. [PubMed: 9539209]

See RE. Neural substrates of cocaine-cue associations that trigger relapse. Eur J Pharmacol. 2005; 526:140–146. [PubMed: 16253228]

Smiley JF, Morrell F, Mesulam MM. Cholinergic synapses in human cerebral cortex: an ultrastructural study in serial sections. Exp Neurol. 1997; 144:361–368. [PubMed: 9168836]

Smith Y, Paré J-F, Paré D. Differential innervation of parvalbuminimmunoreactive interneurons of the basolateral amygdaloid complex by cortical and intrinsic inputs. J Comp Neurol. 2000; 416:496–508. [PubMed: 10660880]

Sugita S, Uchimura N, Jiang ZG, North RA. Distinct muscarinic receptors inhibit release of gamma-aminobutyric acid and excitatory amino acids in mammalian brain. Proc Natl Acad Sci U S A. 1991; 88:2608–2611. [PubMed: 1672454]

Author Manuscript Author Manuscript Author Manuscript Author Manuscript

Szabo, G.; Holderith, N.; Erdelyi, G.; Szabo, G.; Hajos, N. Program No. 423.11. 2009, Neuroscience meeting planner. Washington, DC: Society for Neuroscience; 2009. Cholinergic receptor activation differentially regulates GABA release from parvalbumin- and cholecystokinin-expressing perisomatic inhibitory cells in the basolateral amygdala. Online

Usdin TB, Eiden LE, Bonner TI, Erickson JD. Molecular biology of the vesicular ACh transporter. Trends Neurosci. 1995; 18:218–224. [PubMed: 7610492]

Van Haeften T, Wouterlood FG. Neuroanatomical tracing at high resolution. J Neurosci Methods. 2000; 103:107–116. [PubMed: 11074100]

Vazdarjanova A, McGaugh JL. Basolateral amygdala is involved in modulating consolidation of memory for classical fear conditioning. J Neurosci. 1999; 19:6615–6622. [PubMed: 10414989]

Vizi ES, Kiss JP. Neurochemistry and pharmacology of the major hippocampal transmitter systems: synaptic and nonsynaptic interactions. Hippocampus. 1998; 8:566–607. [PubMed: 9882017]

von Engelhardt J, Eliava M, Meyer AH, Rozov A, Monyer H. Functional characterization of intrinsic cholinergic interneurons in the cortex. J Neurosci. 2007; 27:5633–5642. [PubMed: 17522308]

Wainer BH, Bolam JP, Freund TF, Henderson Z, Totterdell S, Smith AD. Cholinergic synapses in the rat brain: a correlated light and electron microscopic immunohistochemical study employing a monoclonal antibody against choline acetyltransferase. Brain Res. 1984; 308:69–76. [PubMed: 6478204]

Washburn MS, Moises HC. Muscarinic responses of rat basolateral amygdaloid neurons recorded in vitro. J Physiol. 1992; 449:121–154. [PubMed: 1522506]

Weihe E, Tao-Cheng JH, Schäfer MK, Erickson JD, Eiden LE. Visualization of the vesicular acetylcholine transporter in cholinergic nerve terminals and its targeting to a specific population of small synaptic vesicles. Proc Natl Acad Sci U S A. 1996; 93:3547–5352. [PubMed: 8622973]

Womble MD, Moises HC. Muscarinic inhibition of M-current and a potassium leak conductance in neurones of the rat basolateral amygdala. J Physiol. 1992; 457:93–114. [PubMed: 1338469]

Womble MD, Moises HC. Muscarinic modulation of conductances underlying the afterhyperpolarization in neurons of the rat basolateral amygdala. Brain Res. 1993; 621:87–96. [PubMed: 8221077]

Woodruff AR, Sah P. Networks of parvalbumin-positive interneurons in the basolateral amygdala. J Neurosci. 2007a; 27:553–563. [PubMed: 17234587]

Woodruff AR, Sah P. Inhibition and synchronization of basal amygdala principal neuron spiking by parvalbumin-positive interneurons. J Neurophysiol. 2007b; 98:2956–2961. [PubMed: 17715201]

Yajeya J, de la Fuente Juan A, Merchan MA, Riolobos AS, Heredia M, Criado JM. Cholinergic responses of morphologically and electrophysiologically characterized neurons of the basolateral complex in rat amygdala slices. Neuroscience. 1997; 78:731–743. [PubMed: 9153654]

Yajeya J, de la Fuente Juan A, Bajo VM, Riolobos AS, Heredia M, Criado JM. Muscarinic activation of a non-selective cationic conductance in pyramidal neurons in rat basolateral amygdala. Neuroscience. 1999; 88:159–167. [PubMed: 10051197]

Yajeya J, De La Fuente A, Criado JM, Bajo V, Sánchez-Riolobos A, Heredia M. Muscarinic agonist carbachol depresses excitatory synaptic transmission in the rat basolateral amygdala in vitro. Synapse. 2000; 38:151–160. [PubMed: 11018789]

Zaborszky L, Pang K, Somogyi J, Nadasdy Z, Kallo I. The basal forebrain corticopetal system revisited. Ann N Y Acad Sci. 1999; 877:339–367. [PubMed: 10415658]

Zhu PJ, Stewart RR, McIntosh JM, Weight FF. Activation of nicotinic acetylcholine receptors increases the frequency of spontaneous GABAergic IPSCs in rat basolateral amygdala neurons. J Neurophysiol. 2005; 94:3081–3091. [PubMed: 16033935]

Author Manuscript Author Manuscript Author Manuscript Author Manuscript

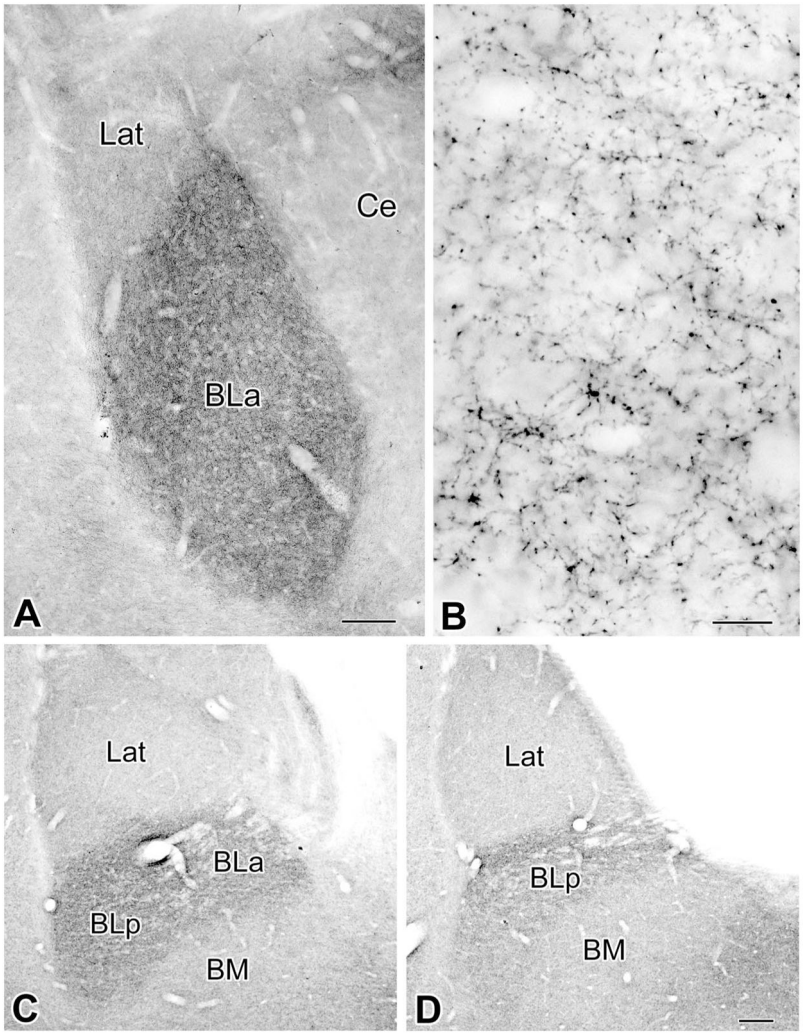

Figure 1.

Innervation of the amygdala by cholinergic VAChT^{+} axons. **A**: Low-power light micrograph of VAChT immunoreactivity at the Bregma –2.3 level (Paxinos and Watson, 1997). Note that the density of VAChT^{+} axons in the BLa is much greater than in the lateral nucleus (Lat) and that the lateral subdivision of the central nucleus (Ce) contains very few VAChT^{+} axons. **B**: Higher power light micrograph of VAChT^{+} axons in the BLa at the level of A. **C,D**: Low-power light micrographs of VAChT immunoreactivity at the Bregma –3.3 level (C) and Bregma –4.0 level (D). Note that the density of VAChT^{+} axons in the BLa and BLp is much greater than in the lateral (Lat) or basomedial nucleus (BM). Scale bars = 150 μm in A; 10 μm in B; 150 μm in D (applies to C,D).

Author Manuscript Author Manuscript Author Manuscript Author Manuscript

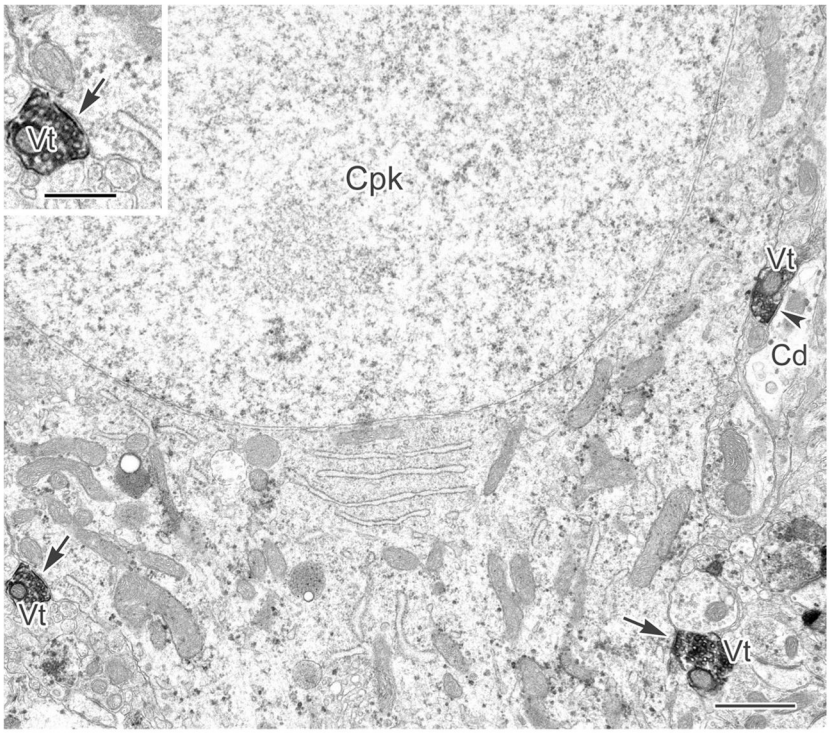

Figure 2.

A CaMK$^+$ pyramidal cell perikaryon (Cpk) labeled with particulate V-VIP reaction product is contacted by three VAChT$^+$ terminals (Vt). Two of these contacts are synaptic (arrows), and the third makes synaptic contact with an adjacent CaMK$^+$ dendrite (Cd, arrowhead). **Inset**: Enlarged view of the synaptic contact (arrow) from the Vt on the left. Scale bars = 1 μm; 0.5 μm in inset.

Author Manuscript Author Manuscript Author Manuscript Author Manuscript

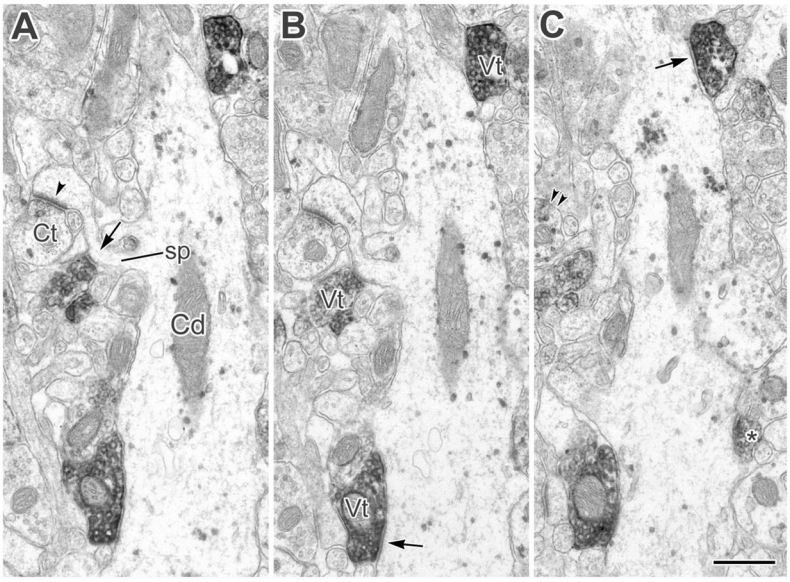

Figure 3.

A–C: A CaMK$^+$ pyramidal cell dendrite (Cd) and its spine (sp, arrow in A) receive multiple synaptic contacts from VAChT$^+$ terminals (Vt, arrows in B,C). The dendritic spine (sp in A), in addition to receiving synaptic input from a VAChT$^+$ terminal (arrow in A), receives an asymmetrical synaptic contact (arrowhead) from a CaMK$^+$ terminal (Ct). The granular V-VIP label for CaMK in the Ct is most apparent in partial view in C (double arrowheads). Another small VAChT$^+$ axonal profile contacting the Cd adjacent to an emerging spine (asterisk in C) appeared synaptic in subsequent sections. A–C are from the first, second, and fourth sections in a short series. Scale bar = 0.5 μm.

Author Manuscript Author Manuscript Author Manuscript Author Manuscript

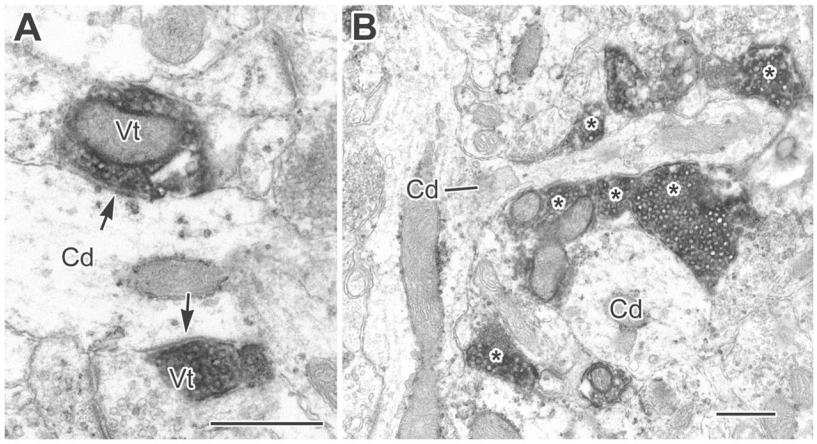

Figure 4.

A: A small-caliber CaMK$^+$ dendrite (Cd) receives synaptic inputs from two VAChT$^+$ terminals (Vt, arrows). **B**: A small-caliber CaMK$^+$ dendrite and its branch (Cd, line) were found, in serial sections, to receive synaptic input from at least six VAChT$^+$ terminals (asterisks). Another CaMK$^+$ dendrite (Cd, lower right) also received several VAChT$^+$ synapses. Scale bars = 0.5 μm.

Author Manuscript Author Manuscript Author Manuscript Author Manuscript

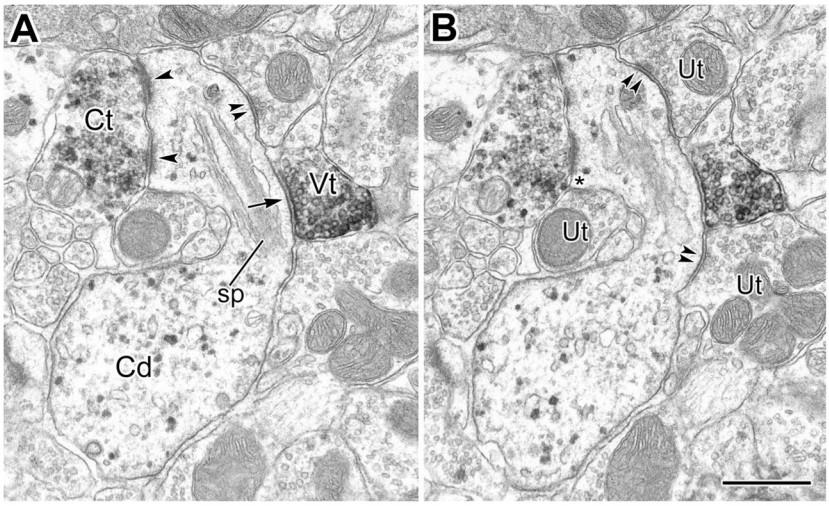

Figure 5.

A,B: Serial electron micrographs of a cross-sectional view of a small-caliber $CaMK^+$ dendrite (Cd) and its spine (sp). A: The spine neck receives a symmetrical synaptic contact from a $VAChT^+$ terminal (Vt, arrow), and the spine head receives a perforated asymmetrical synapse from a $CaMK^+$ terminal (Ct, single arrowheads). The spine also receives symmetrical synaptic contacts from at least two unlabeled terminals (Ut, double arrowheads in A,B), whose small, pleomorphic synaptic vesicles are consistent with their being GABAergic. A third, similar unlabeled terminal appears to be forming a symmetrical synapse onto the spine as well (Ut on left in B, asterisk). Scale bar = 0.5 μm.

Author Manuscript Author Manuscript Author Manuscript Author Manuscript

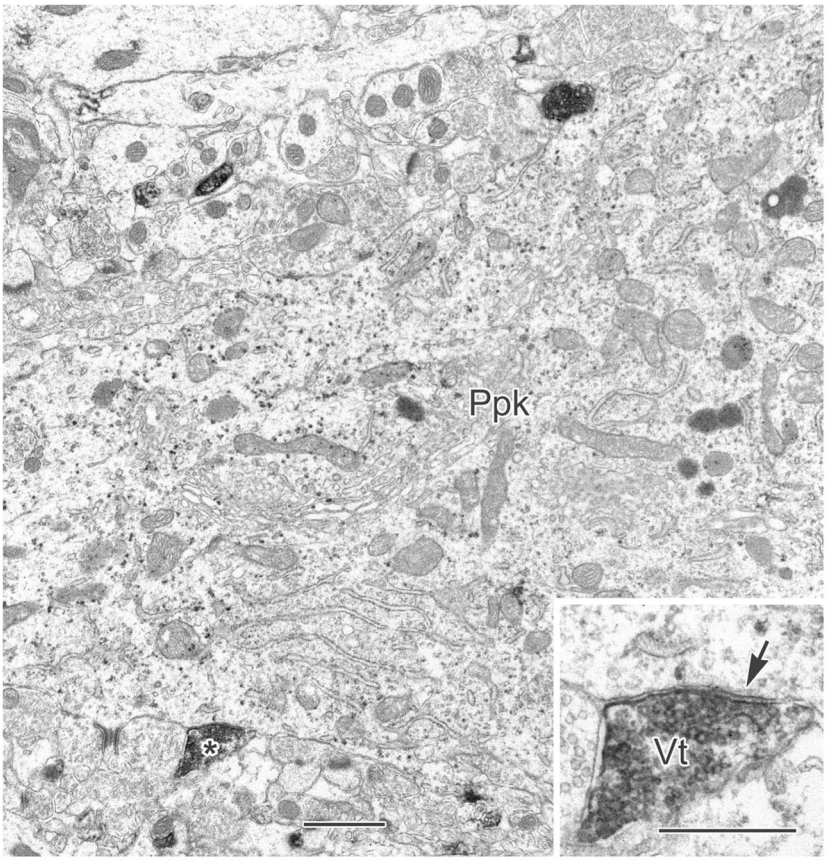

Figure 6.

A V-VIP labeled PV^+ perikaryon (Ppk) receives contacts from two $VAChT^+$ terminals, one of which (asterisk) is clearly synaptic (Vt, arrow in **inset**). Scale bars = 1 μm; 0.5 μm in inset.

Author Manuscript Author Manuscript Author Manuscript Author Manuscript

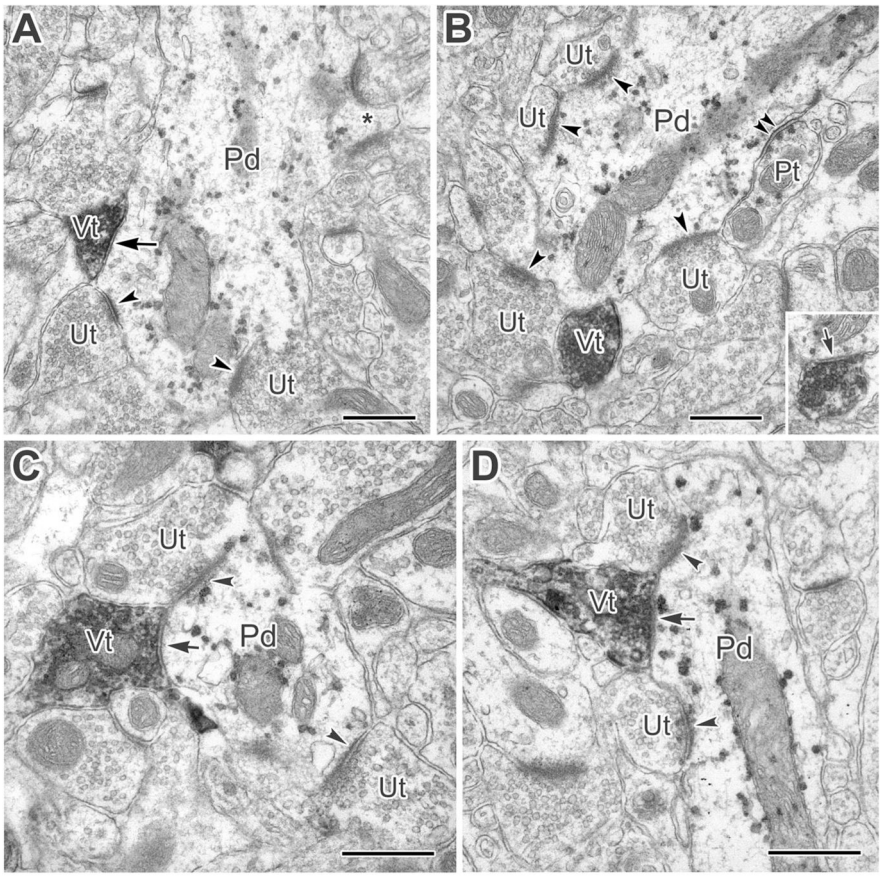

Figure 7.

A: A large-caliber PV^+ dendrite (Pd) receives synaptic input from a $VAChT^+$ terminal (Vt, arrow) as well as asymmetrical synapses from adjacent and nearby unlabeled terminals (Ut, arrowheads). The PV^+ dendrite also gives rise to a spine (asterisk) that receives two asymmetrical synaptic contacts. **B**: A large-caliber PV^+ dendrite receives synaptic contact from a $VAChT^+$ terminal (Vt, arrow in inset). The **inset** is from two thin sections away in the series. This PV^+ dendrite also receives asymmetrical synaptic contacts from four nearby unlabeled terminals (Ut, arrowheads), and a symmetrical synapse from a PV^+ terminal (Pt, double arrowheads). **C**: A small-caliber PV^+ dendrite (Pd) receives synaptic input from a $VAChT^+$ terminal (Vt, arrow). Adjacent and nearby unlabeled terminals (Ut) are shown making asymmetrical synapses (arrowheads). From serial sections, it was found that two more unlabeled terminals formed asymmetrical synapses in the same cross-sectional area as the $VAChT^+$ terminal. **D**: A $VAChT^+$ terminal (Vt) is synapsing onto a PV^+ longitudinally oriented small-caliber dendrite (Pd, arrow). The synapse is oblique in this section but was confirmed in serial sections. The $VAChT^+$ terminal sits between two unlabeled terminals making asymmetrical synapses with the PV^+ dendrite. Scale bars = 0.5 μm.

Author Manuscript

Author Manuscript

Author Manuscript

Author Manuscript

TABLE 1

Primary Antibodies

Antigen	Immunogen	Manufacturing details	Dilution
VAChT	Synthetic peptide, aa 511–530 from cloned rat VAChT	Immunostar, goat polyclonal, catalog No. 24286	1:10,000
Parvalbumin	Rat muscle parvalbumin	Gift from Dr. Kenneth Baimbridge, rabbit polyclonal, antiserum R-301	1:6,000
CaM kinase II	Purified type II CaM kinase alpha 2 subunit	Sigma, mouse monoclonal, catalog No. C265 (clone 6G9)	1:500

Author Manuscript Author Manuscript Author Manuscript Author Manuscript

TABLE 2

Postsynaptic Targets of VAChT$^+$ Axon Terminals in the BLa in VAChT/CaMK Cases[1]

Case	CaMK$^+$ perikarya	CaMK$^+$ LD	CaMK$^+$ SD	Spine	Unlabeled perikarya	Unlabeled LD	Unlabeled SD	Total
EM86	1 (1.5%)	3 (4.5%)	27 (40.3%)	29 (43.3%)	0 (0.0%)	0 (0.0%)	7 (10.4%)	67 (100%)
EM88	3 (3.5%)	7 (8.2%)	35 (41.2%)	31 (36.5%)	0 (0.0%)	0 (0.0%)	9 (10.6%)	85 (100%)
Combined	4 (2.6%)	10 (6.6%)	62 (40.8%)	60 (39.5%)	0 (0.0%)	0 (0.0%)	16 (10.5%)	152 (100%)

[1] LD, large-caliber dendrite; SD, small-caliber dendrite.

Author Manuscript Author Manuscript Author Manuscript Author Manuscript

TABLE 3

Postsynaptic Targets of VAChT^{+} Axon Terminals in the BLa in VAChT/PV Cases[1]

Case	PV^{+} perikarya	PV^{+} LD	PV^{+} SD	Unlabeled perikarya	Unlabeled LD	Unlabeled SD	Unlabeled spine	Total
EM83	0 (0.0%)	2 (2.2%)	4 (4.5%)	6 (6.7%)	6 (6.7%)	40 (44.9%)	31 (34.8%)	89 (100%)
EM87	0 (0.0%)	0 (0.0%)	6 (6.8%)	5 (5.7%)	5 (5.7%)	35 (39.8%)	37 (42.0%)	88 (100%)
Combined	0 (0.0%)	2 (1.1%)	10 (5.6%)	11 (6.2%)	11 (6.2%)	75 (42.4%)	68 (38.4%)	177 (100%)

[1]LD, large-caliber dendrite; SD, small-caliber dendrite.